Journal of Molecular Catalysis A: Chemical 193 (2003) 177–184

JOURNAL OF MOLECULAR CATALYSIS A: CHEMICAL

www.elsevier.com/locate/molcata

Reforming of methane with oxygen and carbon dioxide to produce syngas over a novel $Pt/CoAl_2O_4/Al_2O_3$ catalyst

Liuye Mo[a], Jinhua Fei[a], Chuanjing Huang[b], Xiaoming Zheng[a,*]

[a] *Institute of Catalysis, Zhejiang University (xixi campus), Hangzhou 310028, PR China*

[b] *Department of Chemistry, Huaibei Coal Industry Teacher's College, Huaibei 235000, PR China*

Received 23 April 2002; accepted 24 July 2002

Abstract

$Pt/CoAl_2O_4/Al_2O_3$, $Pt/CoO_x/Al_2O_3$, $CoAl_2O_4/Al_2O_3$ and CoO_x/Al_2O_3 catalysts were studied for combination CO_2 reforming and partial oxidation of CH_4. The results indicate that $Pt/CoAl_2O_4/Al_2O_3$ is more effective, and XRD results indicate that Pt species are well dispersed over the $Pt/CoAl_2O_4/Al_2O_3$. High dispersion is related to the presence of $CoAl_2O_4$, formed during calcining at high temperature before Pt addition. In the presence of Pt, $CoAl_2O_4$ in the catalyst could be reduced partially at 973 K. Based on these results, it appears that zerovalent platinum with high dispersion and zerovalent cobalt resulting from $CoAl_2O_4$ reduction are responsible for high activity in the $Pt/CoAl_2O_4/Al_2O_3$ catalyst.

Keywords: Combination CO_2 reforming and partial oxidation of CH_4; Syngas; $Pt/CoAl_2O_4/Al_2O_3$; Catalyst

1. Introduction

The reforming of methane with carbon dioxide has recently received an increasing interest as it can produce syngas with a H_2/CO ratio around 1, which is suitable for production of methanol and the Fischer–Tropsch synthesis [1–6]. This reaction also has important environmental implications since both methane and carbon dioxide are greenhouse gases. However, this process is highly endothermic and hence, highly energy intensive. The catalytic partial oxidation of methane to synthesis gas may lead to "hot-spot" which is hazardous and/or difficult to control particularly for large-scale operation. Because the CO_2 reforming of methane is an endothermic process, its coupling with the catalytic partial oxidation of methane can overcome the overheating hazard. In addition, by combining the two reactions, one can control the ratio H_2/CO and thus the selectivity for various Fischer–Tropsch synthesis products. This coupling was studied over noble metal-based catalysts [7,8], and nickel-based catalysts [9–11].

In this paper, we report a novel catalyst $Pt/CoAl_2O_4/Al_2O_3$ which is highly active for combination of CO_2 reforming and partial oxidation of CH_4 to syngas.

2. Experimental

2.1. Catalyst preparation

CoO_x/Al_2O_3 and $CoAl_2O_4/Al_2O_3$ catalysts were prepared by the wet-impregnation method, using nitrate salt as the metal precursor and γ-Al_2O_3 as support. After drying at 393 K, the resulting material was then calcined in air at 923 and 1473 K

---

[*] Corresponding author.

1381-1169/02/$ – see front matter © 2002 Elsevier Science B.V. All rights reserved.
PII: S1381-1169(02)00453-3

for 5 h, respectively. The Co loading was 4 wt.% (unless otherwise stated). Pt/CoO_x/Al_2O_3 and Pt/$CoAl_2O_4/Al_2O_3$ catalysts were prepared by impregnating CoO/Al_2O_3 and $CoAl_2O_4/Al_2O_3$ with a solution of H_2PtCl_6 and calcined at 923 K for 5 h. For reference, Pt/Al_2O_3catalysts were also prepared according to the procedure for Pt/$CoAl_2O_4/Al_2O_3$ catalysts, but the carrier (γ-Al_2O_3) was calcined at 1473 K for 5 h before used.

2.2. Catalytic reaction

The catalytic reaction was carried out in a tubular fixed bed flow reactor made of quartz (i.d. = 4 mm) under atmospheric pressure. Prior to reaction, the catalyst was reduced at 973 K in H_2 for 1 h (unless otherwise stated), followed by Ar purge and heating under Ar flow to the reaction temperature (1023 K). The reactant gas stream consisted of methane, carbon dioxide and oxygen with a molar ratio of 1:0.4:0.3 (unless otherwise stated), controlled by mass flow controller, with GHSV = 24 000 h^{-1}. After condensing and drying, the reaction effluents were analyzed using the TCD of a gas chromatography equipped with a TDX-01 column. It must be noted that O_2 was all consumption in all case. The conversion and the selectivity are calculated based on following equations:

$$X(CH_4)\ (\%) = \left(\frac{F(CH_{4,in}) - F(CH_{4,out})}{F(CH_{4,in})}\right) \times 100\%$$

$$X(CO_2)\ (\%) = \left(\frac{F(CO_{2,in}) - F(CO_{2,out})}{F(CO_{2,in})}\right) \times 100\%$$

$$S(H_2) = \left(\frac{F(H_{2,out})}{2(F(CH_{4,in}) - F(CH_{4,out}))}\right) \times 100\%$$

$$S(CO) = \left(\frac{F(CO_{2,out})}{(F(CH_{4,in}) - F(CH_{4,out})) + (F(CO_{2,in}) - F(CO_{2,out}))}\right) \times 100\%$$

$$F_i = F_{total}\, C_i$$

where X, S, F and C_i is conversion, selectivity, gas flow rate and molar fraction of i in the feed gas or the effluent gas, respectively.

2.3. Catalyst characterization

Surface area of the support as well as the catalysts were determined by adsorption at 77 K using the BET method in an OMNISORP 100CX apparatus.

XRD data were obtained using a Rigaku-D/max-B automated power X-ray diffractometer (Cu Kα, 45 kV, 40 mA).

In TPR experiments, 50 mg of catalyst was charged in a quartz micro reactor (i.d. = 4 mm). After purging with N_2 at room temperature, the sample was reduced in a 5% H_2/N_2 stream (30 ml/min). The reaction temperature was uniformly raised with ramp of 20 K/min from room temperature to a holding temperature of 1173 K, which was held for 13 min. The H_2 consumption was monitored by a TCD connected to PC data station.

3. Results and discussion

3.1. Catalytic activity measurements

Table 1 reports the results obtained over various CoO_x/Al_2O_3 catalysts after a reaction time of 0.5 h. It shows that the CoO_x/Al_2O_3 catalyst has poor activity and low selectivity. $CoAl_2O_4/Al_2O_3$ showed only total oxidation of CH_4 until the prereduction temperature was increased to 1123 K. Interestingly, when $CoAl_2O_4/Al_2O_3$ catalyst was reduced at 1123 K, the catalytic activity increased remarkedly. This is attributed to Co metal produced by partially reduction of $CoAl_2O_4$ [12]. Carbon is not formed on the active

Table 1
Catalytic activities of CoO_x/Al_2O_3, $CoAl_2O_4/Al_2O_3$, 0.2% Pt/CoO_x/Al_2O_3, and 0.2% Pt/$CoAl_2O_4/Al_2O_3$

Catalyst	Conversion (%)		Selectivity (%)	
	CH_4	CO_2	H_2	CO
CoO_x/Al_2O_3	32.5	8.0	56.5	98.8
$CoAl_2O_4/Al_2O_3$[a]	–	–	Trace	
$CoAl_2O_4/Al_2O_3$[b]	53.8	35.0	85.4	100
0.2% Pt/ CoO_x/Al_2O_3	52.1	30.5	82.7	100
0.2% Pt/$CoAl_2O_4/Al_2O_3$	80.9	74.5	96.7	99.9

Reaction conditions: $T = 1023$ K, GHSV = 24 000 h^{-1}, $t = 0.5$ h, $CH_4:CO_2:O_2 = 1:0.4:0.3$.

[a] CH_4 combustion primary reaction.

[b] Reduced at 1123 K for 1 h before reaction.

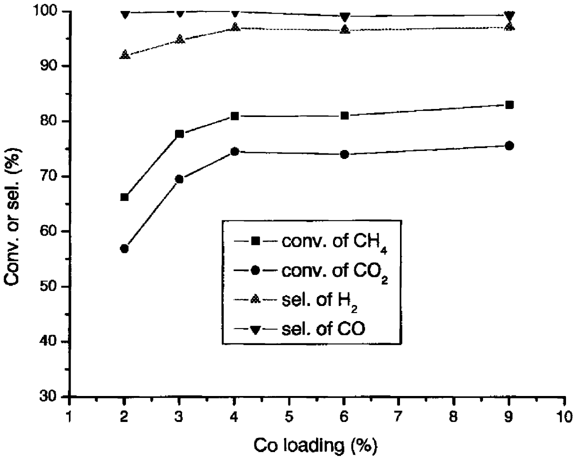

Fig. 1. Effect cobalt loading on catalytic activity of 0.2% Pt/CoAl$_2$O$_3$/Al$_2$O$_3$ (reaction conditions: $T = 1023\,K$, GHSV $= 24\,000\,h^{-1}$, CH_4:CO_2:O_2 = 1:0.4:0.3).

catalysts, and the selectivity of CO is almost 100%. From Table 1, it is also found that with promotion by a small amount of Pt, Pt/$CoAl_2O_4$/Al_2O_3 catalyst showed significant improvement in activity.

Fig. 1 shows the effect of Co loading on the activities of 0.2% Pt/$CoAl_2O_4$/Al_2O_3 catalyst. 0.2% Pt/$CoAl_2O_4$/Al_2O_3 catalysts increase in activity with low Co loading, however, above 4%, increasing Co loading has little effect on the activity. From Fig. 2 it can be seen the effect of Pt content on the activities of Pt/$CoAl_2O_4$/Al_2O_3 catalyst. The changing trend is similar to Fig. 1. As the Pt loading is above 0.1%, the catalytic activities do not increase with increasing the Pt content.

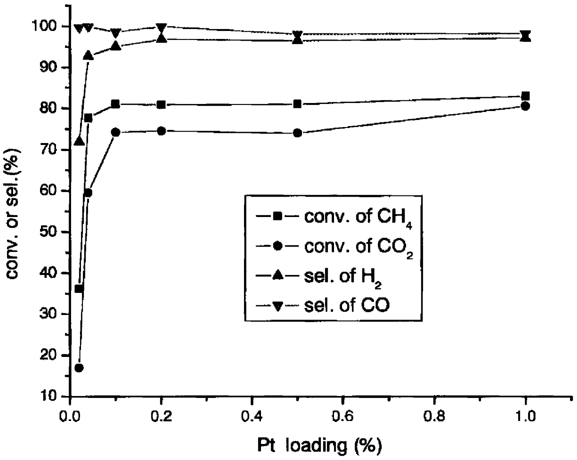

Fig. 2. Effect Pt loading on the catalytic activity of Pt/$CoAl_2O_4$/Al_2O_3 (reaction conditions: $T = 1023\,K$, GVSV $= 24\,000\,h^{-1}$, CH_4:CO_2:O_2 = 1:0.4:0.3).

Fig. 3 shows the effect of reaction temperature on the catalytic activity of 0.2% Pt/$CoAl_2O_4$/Al_2O_3 catalyst. It shows that the conversion of CH_4 and CO_2 and the selectivity of H_2 increase with increasing reaction temperature, but the selectivity of CO is not affected by reaction temperature. This result is identical with thermodynamic of this reaction.

The effect of reactant gas ratio on the catalytic activity is examined in Fig. 4. Clearly, the conversion of CH_4 increased monotonically with increasing O_2/CO_2 ratio, while the selectivity of H_2 decreased slightly as increasing O_2/CO_2 ratio, while the selectivity of CO remained almost unchanged at about 99%. More important, the H_2/CO ratio varied from 1.05 to 1.68 as O_2/CO_2 ratio increased from 0.1 to 2.0. It can be deduced that H_2/CO ratio can be adjusted from 1.0 to 2.0 if the reactant gas follows the equation $FCH_4 = FCO_2 + 2FO_2$. It can be seen that by combining the two reactions, one can control the ratio H_2/CO and thus the selectivity for various Fischer–Tropsch synthesis products.

Catalyst stability was also examined. Fig. 5 shows that a rapid decline in CH_4 conversion is observed for the 0.2% Pt/Al_2O_3 catalyst. During 2 h of reaction, the conversion of methane decreases from 40.1% for the initial reaction to 31.2%. The deactivation reason of 0.2% Pt/Al_2O_3 catalyst is not attributed to carbon deposition (the carbon amount was too small to be detected by TPO), but attributed to the sinter of Pt. The crystalline size of Pt detected by XRD using fundamental parameters approach [13] is 32.6 and 49.59 nm for fresh and used catalyst, respectively. However, 0.2% Pt/$CoAl_2O_4$/Al_2O_3 catalyst maintains its high activity during 30 h on stream without coke formation, showing superior stability.

3.2. XRD study

Fig. 6 shows XRD spectra of CoO_x/Al_2O_3 catalysts and $CoAl_2O_4$/Al_2O_3 which were calcined at 923 and 1473 K, respectively. For CoO_x/Al_2O_3 catalysts, three peaks are observed at d = 0.244, 0.286 and 0.467 nm (2θ-value: 36.8, 31.3 and 19.0°, respectively).

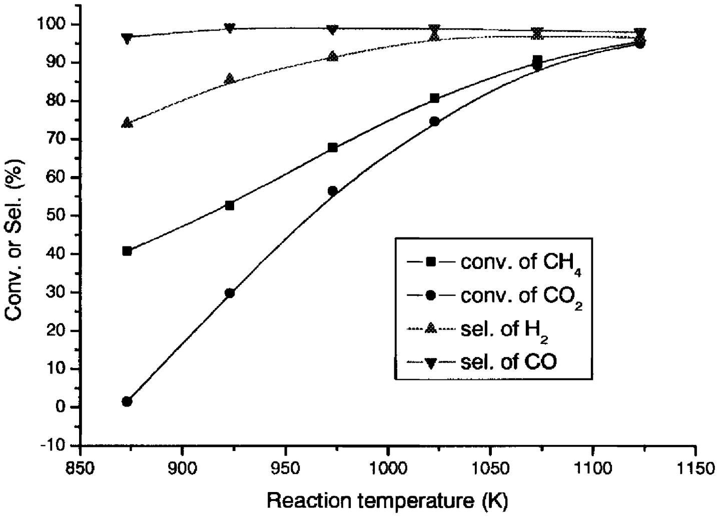

Fig. 3. Effect of reaction temperature on catalytic activity of 0.2% Pt/$CoAl_2O_4/Al_2O_3$ (reaction conditions: $T = 1023\,K$, GHSV $= 24\,000\,h^{-1}$, $CH_4:CO_2:O_2 = 1:0.4:0.3$).

Considering that the diffraction lines characteristic of Co_3O_4 and $CoAl_2O_4$ blend together at $d = 0.244$ and 0.286 nm, except for a line of Co_3O_4 at 0.476 nm which is absent from XRD pattern of $CoAl_2O_4$ [12], the presence of Co_3O_4 is suggested for the CoO_x/Al_2O_3 catalyst. With $CoAl_2O_4/Al_2O_3$, however, the peak at 0.467 nm disappears and several sharp peaks clearly exhibit the presence of $CoAl_2O_4$ and α-Al_2O_3, agreeing with the literature [2]. This is also supported by the results in Table 2. When calcination temperature was increased from 923 to 1473 K, the catalyst experienced pronounced changes in color

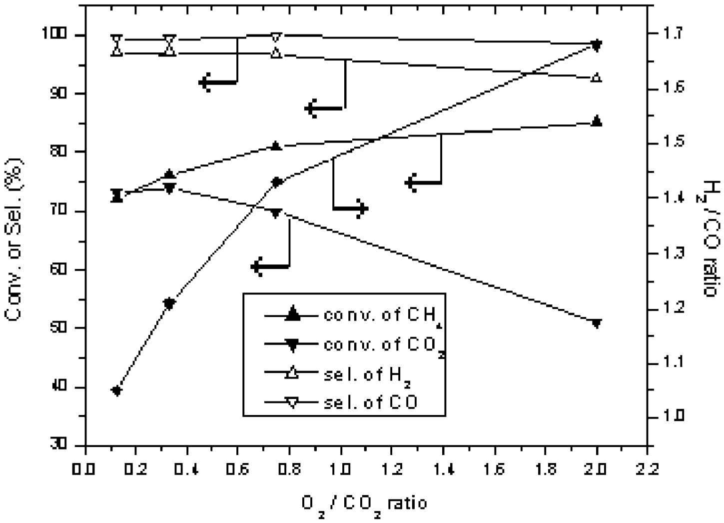

Fig. 4. Effect O_2/CO_2 ratio on the catalytic activity and the ratio of H_2/CO (reaction conditions: $T = 1023\,K$, GSVH $= 24\,000\,h^{-1}$, reactant gas ratio: $FCH_4 = FCO_2 + 2FO_2$).

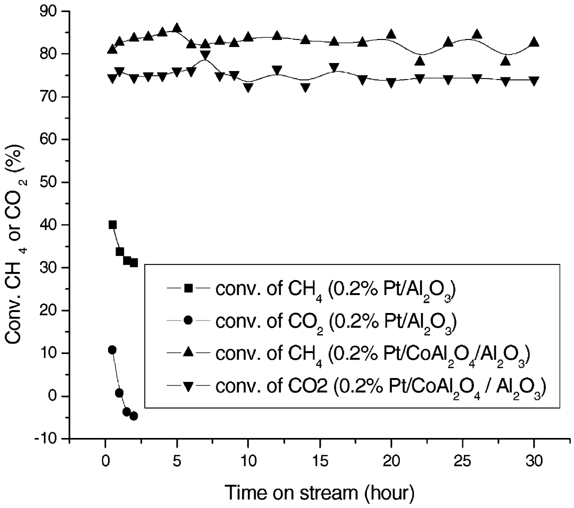

Fig. 5. Stability of catalysts for combination of CO_2 reforming and partial oxidation of CH_4 (reaction conditions: $T = 1023$ K, GHSV = 24 000 h^{-1}, CH_4:CO_2:O_2 = 1:0.4:0.3).

and surface area, indicating phase transformations of Co_3O_4 to $CoAl_2O_4$ and γ-Al_2O_3 to α-Al_2O_3.

The effect of platinum addition on XRD patterns for CoO_x/Al_2O_3 and $CoAl_2O_4/Al_2O_3$ catalysts is shown in Fig. 7. When the loading of Pt is 1%, crystalline PtO_2 is clearly detected for Pt/Al_2O_3 and Pt/CoO/Al_2O_3 catalysts. However, no distinct XRD peaks of Pt species are detected for Pt/$CoAl_2O_4/Al_2O_3$ catalysts at 1% Pt, although weak peaks of PtO_2 are observed at 2% Pt. These findings suggest that Pt species are highly dispersed in the Pt/$CoAl_2O_4/Al_2O_3$ catalyst.

Table 2
Color and surface area of catalysts

Catalyst	Color	BET area (m^2/g)
Al_2O_3[a]	White	162.9
Pt/Al_2O_3[b]	White	8.8
CoO_x/Al_2O_3	Black	162.9
$CoAl_2O_4/Al_2O_3$	Sky blue	8.6
0.2% Pt/CoO_x/Al_2O_3	Black	153.1
0.2% Pt/$CoAl_2O_4/Al_2O_3$	Sky blue	9.9

[a] Calcined at 923 K.

[b] Al_2O_3 was precalcined at 1473 K.

Fig. 8 shows that crystalline $CoAl_2O_4$ is presence in the used (2 h) 0.2% Pt/$CoAl_2O_4/Al_2O_3$ catalyst. This result indicates that the 0.2% Pt/$CoAl_2O_4/Al_2O_3$ catalyst can only be reduced partially under prereduction and reaction condition, which is perhaps attributed to the high activity of 0.2% Pt/$CoAl_2O_4/Al_2O_3$.

3.3. TPR results

From Fig. 9, it can be seen that the reduction behaviors of $CoAl_2O_4/Al_2O_3$ with and without Pt

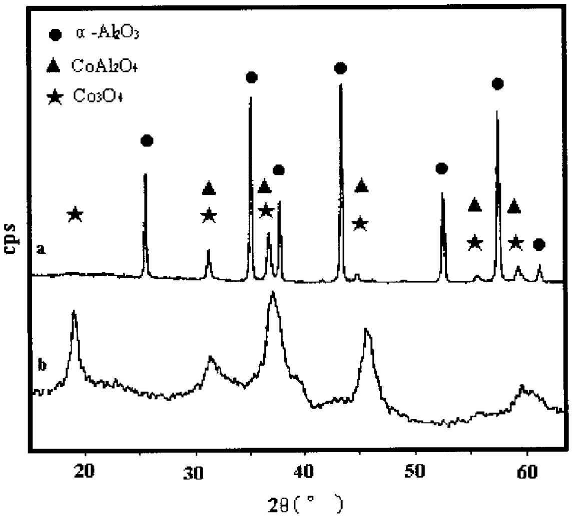

Fig. 6. Patterns of (a) $CoAl_2O_4/Al_2O_3$; (b) CoO_x/Al_2O_3.

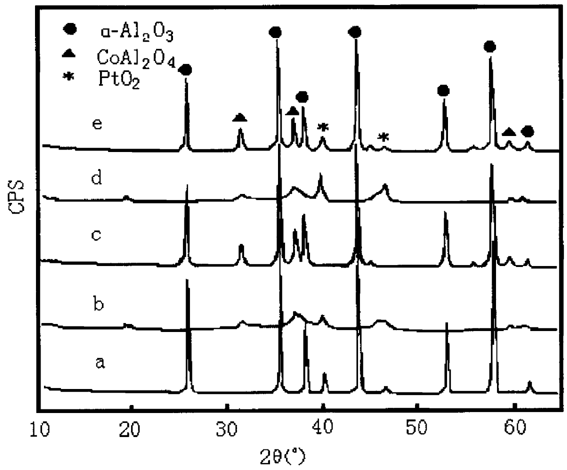

Fig. 7. XRD patterns of Pt/$CoAl_2O_4/Al_2O_3$. (a) 1% Pt/Al_2O_3; (b) 1% Pt/CoO_x/Al_2O_3; (c) 1% Pt/$CoAl_2O_4/Al_2O_3$; (d) 2% PtCoO_x/Al_2O_3; (e) 2% Pt/$CoAl_2O_4/Al_2O_3$.

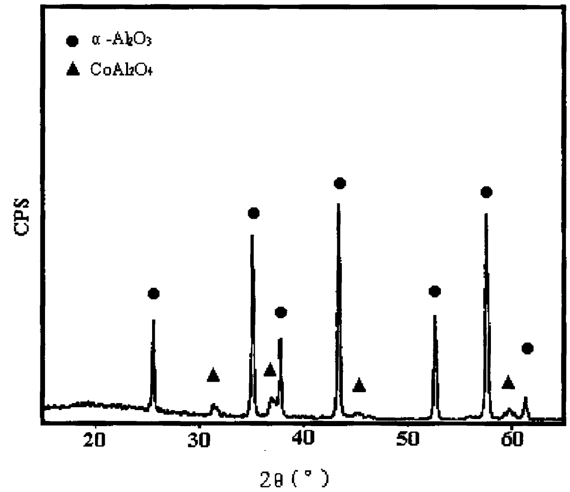

Fig. 8. XRD pattern of 0.2% Pt/$CoAlO_4/Al_2O_3$ (used).

are far different. On $CoAl_2O_4/Al_2O_3$ catalyst a peak due to the reduction of $CoAl_2O_4$ [14] appears above 1173 K. On Pt/Al_2O_3, catalyst three peaks appear at 423, 493 and 713 K, respectively. The former two peaks could be assigned to a two-step reduction of "free" PtO_2 [15], i.e. $Pt^{4+} \rightarrow Pt^{2+} \rightarrow Pt^0$, and the last peak probably indicates stronger interaction with the support. These peaks are also observed for Pt/$CoAl_2O_4/Al_2O_3$ catalysts. However, due to Pt addition, the peak of CoO_x/Al_2O_3 reduction shifts to about 1100 K and its intensity is greatly increased. This clearly demonstrates that Pt promotes reduction of $CoAl_2O_4$. The Pt-assisted process could be attributed to hydrogen spillover, which facilitates $CoAl_2O_4$ reduction. Fig. 10 shows TPR profiles of $CoAl_2O_4/Al_2O_3$ and catalysts that have been reduced at 973 K in H_2 for 1 h and cooled in N_2 flow after the reduction. It can be seen from Fig. 10 (profile a) that the reduced $CoAl_2O_4/Al_2O_3$ catalyst is the same as that of the fresh one, which indicated that in the $CoAl_2O_4/Al_2O_3$ catalyst cannot be reduced under the pretreatment conditions. On the other hand, by comparing the reduced 0.2% Pt/$CoAl_2O_4/Al_2O_3$ catalyst (profile b) with the fresh 0.2% Pt/$CoAl_2O_4/Al_2O_3$ catalyst (profile c) in Fig. 10, it can be found that the reduced one in addition disappears the peaks due to platinum reduction and decreases the area of the peaks for $CoAl_2O_4$ reduction. Based on the hydrogen consumption, it can be calculated that about 31% of the Co, being as $CoAl_2O_4$ in the catalyst, is reduced to Co^0 by reduction at 973 K for 1 h. Fig. 10 profiles show that under prereduction Pt promotes partial reduction of $CoAl_2O_4$, which is also proved by XRD (Fig. 8).

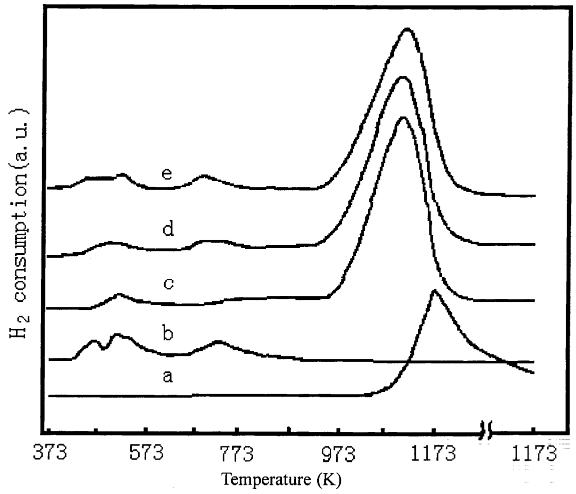

Fig. 9. TPR profiles of (a) $CoAl_2O_4/Al_2O_3$; (b) 1% Pt/Al_2O_3; (c) 0.2% Pt/$CoAl_2O_4/Al_2O_3$; (d) 0.6% Pt/$CoAl_2O_4/Al_2O_3$; (e) 1% Pt/$CoAl_2O_4/Al_2O_3$.

Relating results of TPR and activity measurements listed in Table 1, it appears that the zerovalent platinum and zerovalent cobalt resulting from $CoAl_2O_4$ reduction promoted by Pt are responsible for the high activity of Pt/$CoAl_2O_4/Al_2O_3$ catalysts for combination of CO_2 reforming and partial oxidation of CH_4 to syngas. In addition, the remained $CoAl_2O_4$ in the catalyst probably plays a role in the suppression of coking during reaction. This is supported by the results obtained over Ni/Al_2O_3 [16]and Co/Al_2O_3 [2] catalyst.

As shown in Fig. 11, the Pt-assisted reduction of Co species is also observed for Pt/CoO_x/Al_2O_3 catalysts. On CoO_x/Al_2O_3 catalysts, two peaks appear at 863 and 1173 K, which are ascribed to the reduction of Co_3O_4 and cobalt surface phase, respectively. With addition of a small amount of Pt, the peaks shift to lower temperature. However, it can be seen from Table 2 that in the case of catalytic performance, the effect of Pt addition is far different for CoO_x/Al_2O_3 and $CoAl_2O_4/Al_2O_3$ catalysts.

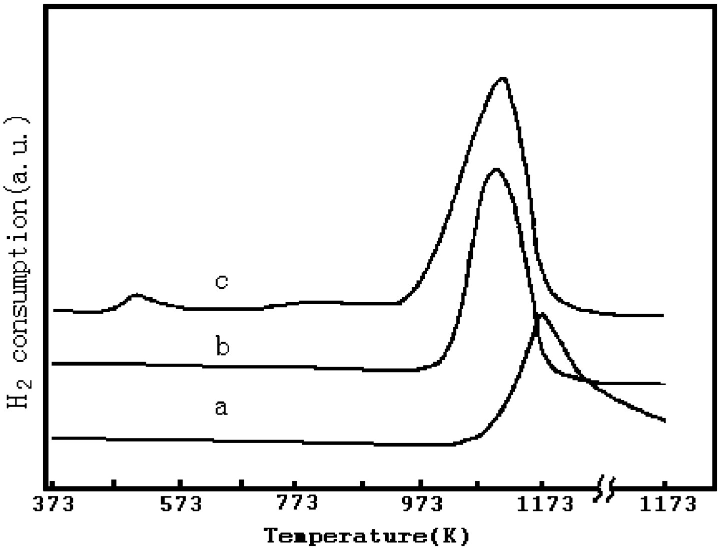

Fig. 10. TPR profiles of $CoAl_2O_4/Al_2O_3$ and 0.2% $Pt/CoAl_2O_4/Al_2O_3$ catalysts before and after reduction at 973 K for 1 h. (a) $CoAl_2O_4/Al_2O_3$ before or after reduction; (b) 0.2% $Pt/CoAl_2O_4/Al_2O_3$ after reduction; (c) 0.2% $Pt/CoAl_2O_4/Al_2O_3$ before reduction.

As to the great difference in activity between 0.2% $Pt/CoO_x/Al_2O_3$ and 0.2% $Pt/CoAl_2O_4/Al_2O_3$ catalysts (see Table 1), the other clue probably lies in the different dispersion of PtO_2, the precursor of Pt^0, over the two catalysts suggested by the XRD results shown in Fig. 7. It is probable that a higher dispersion of PtO_2 is likely to result in a higher dispersion of Pt^0, which is responsible for higher activity. This is supported by literature for $Pt\text{-}Co/Al_2O_3$ catalyst [17].

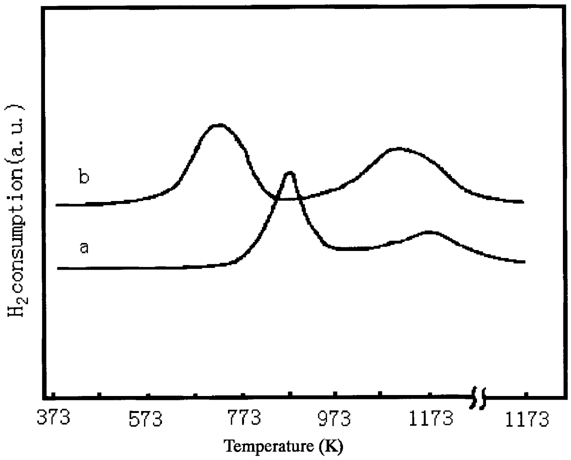

Fig. 11. TPR profiles of (a) CoO_x/Al_2O_3; (b) 0.2% $Pt/CoO_x/Al_2O_3$.

4. Conclusions

The combination of CO_2 reforming and partial oxidation of CH_4 has been investigated on $Pt/CoO_x/Al_2O_3$ and $Pt/CoAl_2O_4/Al_2O_3$ catalysts by comparing with CoO_x/Al_2O_3, $CoAl_2O_4/Al_2O_3$ and Pt/Al_2O_3 catalysts. Among the catalysts investigated, $CoAl_2O_4/Al_2O_3$ calcined at 1473 K and promoted by a small amount of Pt is the most effective for the combination of CO_2 reforming and partial oxidation of methane, in terms of high activity, optimal stability and excellent resistance to carbon deposition. At lower metal content, the activity order for the catalysts is $Pt/CoAl_2O_4/Al_2O_3 > Pt/CoO_x/Al_2O_3 > Pt/Al_2O_3 \gg CoAl_2O_4/Al_2O_3$. Due to Pt addition, $CoAl_2O_4$ in the catalyst can be reduced partially under H_2 at 973 K.

Acknowledgements

We thank the Zhejiang provincial Natural Science Foundation of China for the financial support.

References

[1] A.T. Ashcroft, A.K. Cheetham, M.L. Green, P.D.F. Vernon, Nature 352 (1991) 225.

[2] P.F. Wang, N.C. Wu, X.M. Zheng, J. Catal. (China) 6 (1995) 196.

[3] C.J. Huang, J.H. Fei, D.J. Wang, X.M. Zheng, Chin. Chem. Lett. 3 (2000) 181.

[4] C.J. Huang, X.M. Zheng, L.Y. Mo, J. H Fei, Chin. Chem. Lett. 3 (2001) 249.

[5] C.J. Huang, X.M. Zheng, J.H. Fei, J. Catal. (China) 2 (2001) 138.

[6] C.J. Huang, X.M. Zheng, L.Y. Mo, J.H. Fei, Chin. J. Chem. 4 (2001) 340.

[7] P.D.F. Vernon, M.L. Green, A.K. Cheetham, A.T. Ashcroft, Catal. Today 46 (1998) 203.

[8] A.M. O'Connor, J.R.H. Ross, Catal. Lett. 32 (1998) 203.

[9] V.R. Choudhary, A.M. Rajput, B. Prabhaker, Catal. Lett. 32 (1995) 391.

[10] E. Ruckenstein, Y.H. Hu, Ind. Eng. Chem. Res. 37 (1998) 1744.

[11] V.R. Choudhary, A.S. Mamman, Appl. Energy 66 (2000) 161.

[12] Y. Lu, C. Deng, X. Ding, S.K. Shen, J. Catal. (China) 30 (2000) 85.

[13] R.W. Cheary, A.A. Coelho, J. Appl. Cryst. 25 (1992) 109.

[14] P. Monlijn, J.A. Arnoldy, J. Catal. 93 (1985) 38.

[15] B. Mile, D. Stirling, M.A. Zammitt, A. Lovell, M. Webb, J. Catal. 114 (1988) 217.

[16] Y.G. Chen, J. Renm, Catal. Lett. 29 (1994) 39.

[17] L. Guczi, T. Hoffer, Z. Zso Idos, J. Phys. Chem. 95 (1991) 802.